Emplacement of Olivine-Orthopyroxene-Cr-Spinel- and Sulfide-Bearing Magmas at Jinchuan, Western China.

Sybrand A. de Waal[1], Zhanghua Xu[1], Hassina Mouri[1] and Chusi Li[2]
[1]Department of Geology, University of Pretoria, Republic of South Africa;
[2]Department of Geological Sciences, Indiana University, USA
email: sadw@scientia.up.ac.za

The Jinchuan Ultrabasic Intrusion, Gansu Province, China, hosts a world-class Ni-Cu-PGE sulfide deposit. Chai and Naldrett (1992a and b) gave an overview of the geology and mineralization of this dyke-like body of olivine orthocumulate rocks. They showed that olivine-chromite cumulates predominate, that the primary magma of the Jinchuan intrusion most probably was a high magnesium basalt related to continental magmatism. They suggested that the intrusion represents preserved roots of a large layered intrusion with much of its gabbroic cap being eroded. In contrast, Tang (1998a and b) proposed that the Jinchuan formed from multiple injections of magmas and sulfide liquid from a series of staging chambers. They suggested that the unmineralized rocks against the hangingwall of the dyke formed by the earliest emplacement of magma derived from a relatively deep-seated staging chamber. Successive injections of variable sulfide-bearing magmas and pure sulfide liquid from successively higher-level staging chambers formed disseminated and massive sulfide ores, respectively.

We report on a petrographic and geochemical study (major and trace elements determined by XRF) of 150 samples from the Jinchuan body. The samples are from borehole II14-83 at the central segment of the dyke and from boreholes I14-16 and II48-136, situated towards the east and west of borehole II14-83, respectively (Figure 1). Borehole II14-83 displays a well-defined, symmetrically zoned morphology with sulfide-rich ore in the center. In the other two boreholes the sulfide-enriched rocks are concentrated toward the basal contact.

Petrographic observations indicate that the first mineral to crystallize from the Jinchuan magma was chromium spinel followed by orthopyroxene (Table 1). Both minerals occur as inclusions in cumulus olivine (Fo_{86}) (Figure 2). The mass ratio of orthopyroxene-to-olivine in the original cumulus assemblage is estimated by visual estimation to be below 0.05. This observation is consistent with the result of a Pearce ratio analysis (Pearce, 1989) (Figure 3). Using whole rock compositions corrected for sulfide, H_2O and CO_2, the compositions of olivine, Cr-spinel and orthopyroxene (determined by electron microprobe; chromium spinel from Barnes and Tang, 1998), and our modeled parental magma composition, we calculated the modal cumulus mineral compositions of the rocks by least squares optimization. The results reveal that in the central segment of the intrusion (II14-83) cumulus olivine is concentrated towards the center of the dyke (Figure 4a). This symmetric olivine enrichment distribution is more pronounced when the sulfide fraction is removed (Figure 4b), suggesting that sulfide liquid and trapped silicate melt competed for the same inter-cumulus spaces.

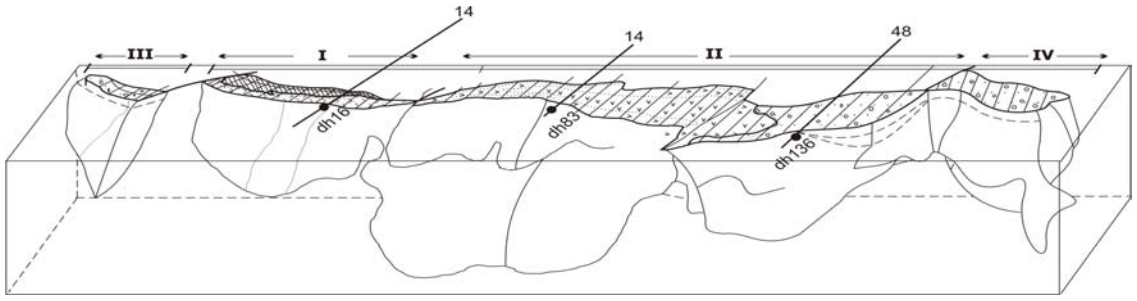

Figure 1. *Oblique 3D view of the Jinchuan Ultrabasic Intrusion. Mining areas I, II, II and IV and the position of the boreholes (black dots) and borehole series (numbered lines) are shown (adapted after Tang, 1995).*

Table 1 *Cations per 6 Oxygen ions in cumulus (A) and interstitial (B) orthopyroxene.*

	A	B		A	B		A	B
Si	1.930	1.916	Fe^{3+}	0.107	0.066	Mn	0.009	0.006
Ti	0.000	0.005	Fe^{2+}	0.246	0.213	Ca	0.003	0.087
Al	0.033	0.081	Ni	0.001	0.001	Na	0.001	0.004
Cr	0.001	0.016	Mg	1.669	1.606	Sum	4.000	4.000

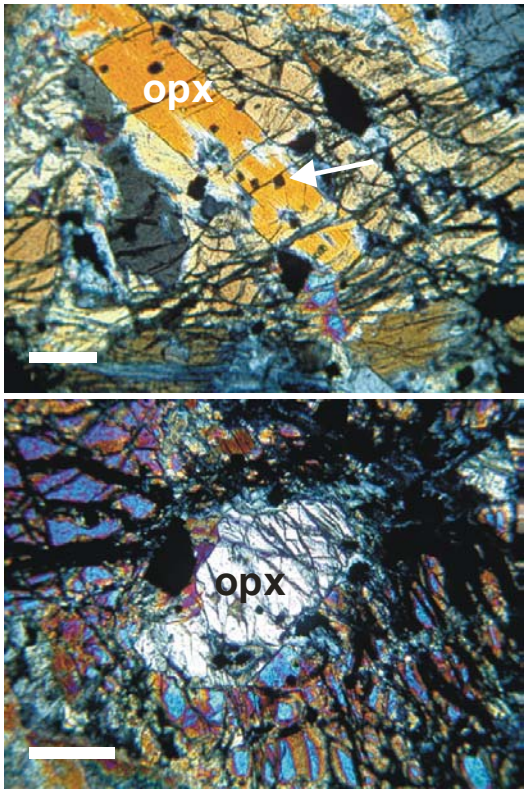

Figure 2*. Orthopyroxene (opx) crystals enclosed in cumulus olivine. Note the chromium spinel (small black spots, arrow) in both orthopyroxene and olivine. Scale bar = 300 µm.*

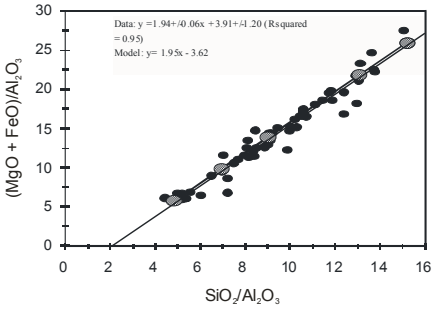

Figure 3. *Pearce ratio diagram comparing the rock data with a model (grey ellipses) assuming olivine + orthopyroxene + chromium spinel as cumulus phases. Orthopyroxene-to-olivine ratio = 0.05, and chromium spinel calculated from Cr content of the rocks.*

At the western and eastern segments of the intrusion (I14-16 and II48-136, respectively) the stratigraphic distribution of cumulus olivine in the whole rock is rather constant, with only minor scattering throughout the boreholes (Figures 5 and 6). Similarly, the modal olivine contents in mineralized samples increase when the sulfide fraction is removed.In borehole II14-83, incompatible trace element concentrations correlate positively with the estimated amounts of trapped silicate liquid (Figure 7). Such correlation is much weaker in the other two boreholes.

Thermodynamic calculations, using MELTS (Ghiorso and Sack, 1995), indicate that orthopyroxene appears on the liquidus of our modeled magma (Cr_2O_3-free) at >~ 5 kbar. At lower pressure, olivine (Fo_{86}) replaces orthopyroxene as the first solid from the magma. The pressure transition is reduced to ~3 kb when the modeled magma of Chai and Naldrett (1992b) is used.

The occurrence of orthopyroxene inclusions in cumulus olivine suggests that crystallization occurred at variable depths at Jinchuan. The incipient crystallization of orthopyroxene probably took place during magma ascent, below 10 to 15 km (3 to 5 kbar). The crystallization of orthopyroxene was succeeded by olivine when the magma moved up into a staging chamber. Sulfide-silicate segregation and sulphide liquid aggregation apparently occurred in this chamber. The highly viscous olivine- and sulfide-laden magmas were then sequentially pumped up to a higher level to form the Jinchuan intrusion. The central part of the intrusion (borehole II14-83) appears to represent the proximal sub-vertical part of an ascending magma conduit in which olivine crystals and sulfide liquid concentrated in the center of the magma flow in response to higher velocity in this regime. The western and eastern parts of the intrusion (boreholes I14-16 and II48-136, respectively) may represent more distal fronts where sub-lateral flow dynamics controlled the observed distribution of rock types. Mingling with earlier magma flows and schlieren formation in these more distal areas are indicated.

References

Barnes, S.J. and Tang, Z., 1998, Chromites from the Jinchuan , Yejili and Zangbutai intrusions, Gansu Province, China, *in* Jiang, X. and Bai, T., eds., Mineralization method of magmatic sulphide deposits: Beijing, Geological Publishing House, p.27-35.

Chai, G. and Naldrett, A.J., 1992a, The Jinchuan Ultramafic Intrusion: cumulate of a high-Mg basaltic magma: J. Petrol., v.33, p.277-303.

Chai, G. and Naldrett, A.J., 1992b, Characteristics of the Ni-Cu-PGE mineralization and genesis of the Jinchuan deposit, northwest China: ECON. GEOL., v.87, p.1475-1495.

Ghiorso, M.S. and Sack, R.O., 1995, Chemical mass transfer in magmatic processes IV. A revised and internally consistent thermodynamic model for the interpolation and extrapolation of liquid-solid equilibria in magmatic systems at elevated temperatures and pressures: Contrib. Min. Petrol., v.119, p.197-212.

Pearce, T.H., 1989, Getting the most from your data: Applications of Pearce Element Ratio Analysis, *in* Russel, J.K and Stanley,C.R., eds., Theory and application of Pearce Element Ratios to geochemical data analysis: Geological Association of Canada, Short course notes 8, p.99-130.

Tang, Z., 1995, Ore-forming model and geological correlation of the Jinchuan CuNi(PGE-bearing) sulfide deposit: Beijing, Geological Publishing House, 208p.

Tang, Z., 1998a, Main mineralization mechanism of magmatic sulphide deposits, *in* Jiang, X. and Bai, T., eds., Mineralization method of magmatic sulphide deposits: Beijing, Geological Publishing House, p.1-9.

Tang, Z., 1998b, Genetic model of the Jinchuan nickel-copper deposit, *in* Jiang, X. and Bai, T., eds., Mineralization method of magmatic sulphide deposits: Beijing, Geological Publishing House, p.10-26.

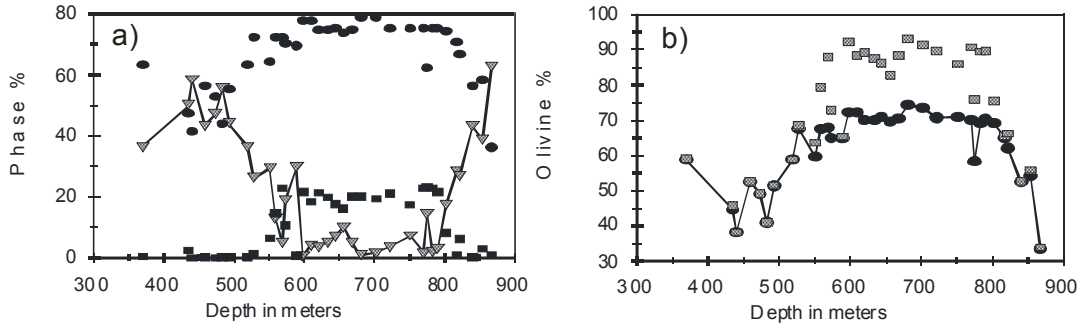

Figure 4. *a)Variation of cumulus minerals (filled dots), interstitial silicate magma (inverted triangles) and sulphide (filled squares) through borehole II14-83. Broad curved pattern are interpreted as flow segregation feature, and sharp, high frequencies variations are seen as schlieren structures; b) Olivine (squares) in silicate fraction (sulfide corrected) compared to olivine (filled dots) in the total rock. In sulfide-rich sections olivine is enriched in the silicate fraction.*

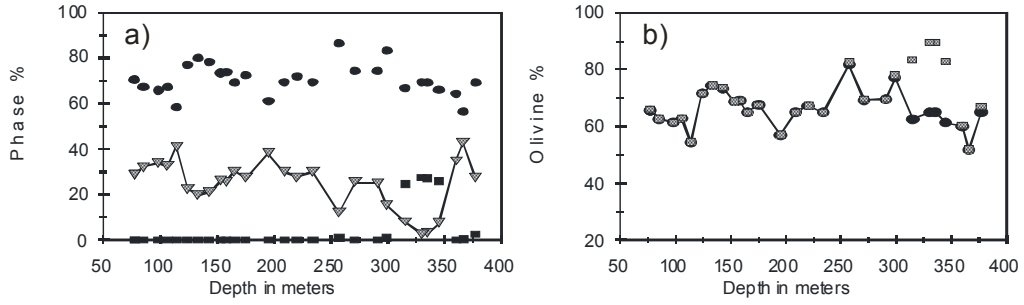

Figure 5. *a) Variation of cumulus minerals (filled dots), interstitial silicate magma (inverted triangles) and sulphide (filled squares) through borehole I14-16. No flow differentiation features recognizable, but schlieren may be present. b) Olivine (squares) in silicate fraction (sulfide corrected) compared to olivine (filled dots) in the total rock.*

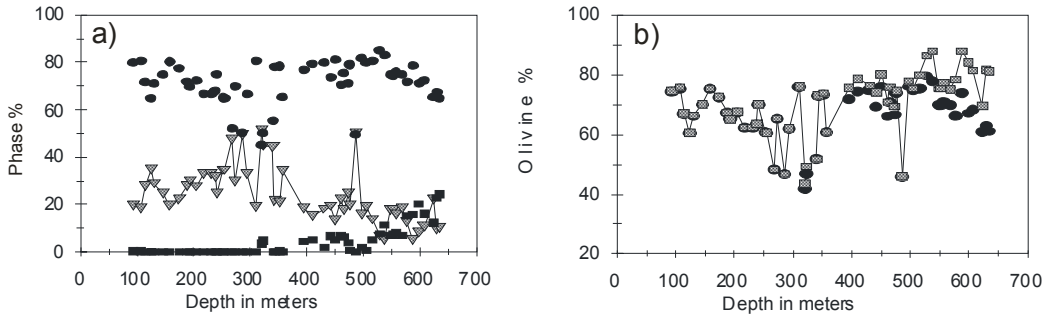

Figure 6. *a) Variation of cumulus minerals (filled dots), interstitial silicate magma (inverted triangles) and sulphide (filled squares) through borehole II48-136. No flow differentiation features recognizable, but abundant schlieren may be present at about 300 meter depth. b) Olivine (squares) in silicate fraction (sulfide corrected) compared to olivine (filled dots) in the total rock.*

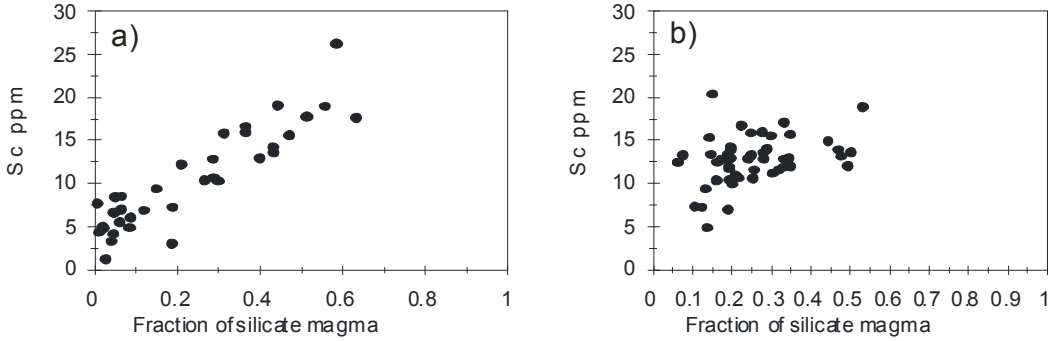

Figure 7. *a) Linear correlation between Sc and the fraction interstitial magma is borne out by the data for borehole II14-83. b) The data for the other two boreholes, here represented by II48-136, do not show this expected strong linear trend. This deviation is interpreted to reflect a more complex mixing history in boreholes I14-16 and II48-136 than in borehole II14-83.*